Restricted ion flow at the nuclear envelope of cardiac myocytes

J. Omar Bustamante

University of Maryland School of Medicine, Departments of Physiology and Medicine, Division of Cardiology-Heart Center, Baltimore, Maryland 21201 USA

ABSTRACT Flow of small ions across the nuclear envelope (NE) is thought to occur without restriction through large diameter nuclear pore complexes (NPCs). However, investigations with electron and fluorescence microscopy, and with patch-clamp and microelectrode electrophysiology, suggest that in many animal and plant cell types small ions move through a barrier having the signature of large conductance nuclear ion channels (NICs). As nucleocytoplasmic transport and gene activity are regulated by cytoplasmic signals and as it has recently been shown by this investigator that cardiac NICs are sensitive to cAMP-dependent processes (1), it was considered relevant to further investigate the effects of various cytosolic signals on NIC activity. Ion species substitution demonstrated that K^+ is the major species responsible for NIC currents. The Na-channel blocker tetrodotoxin (TTX, 100 μM) and the Ca-channel blocker diltiazem (100 μM) had no effect, indicating no relation of NICs to Na- or Ca-channels in transit to the cell surface membrane. Zn^{2+} (100 μM) blocked NIC activity, suggesting a dual role in nucleocytoplasmic transport and gene function. GTP did not produce measurable effect. However, its nonhydrolyzable analogue GTP-γ-S (10 μM) suppressed NIC activity, suggesting a role for GTP hydrolysis in NIC function. Deoxynucleotides (dNTPs, 200 μM) produced a transient increase in NIC activity, pointing to a modulation of NIC function by nucleic acid substrates. These results indicate a role for NICs in mediating: (*a*) control of gene activity by transduction and other cytosolic signals, and (*b*) nuclear demands and response to such signals.

INTRODUCTION

The only way matter is thought to pass between the cell nucleus and the cytoplasm is through the nuclear pores of the NE (2). So far, little attention has been paid to NE electrical properties due to the apparent large effective diameter of NPCs ($\sim$10 nm; 3, 4) which, as a result, are presumed to offer negligible resistance to the flow of small physiological ions like K^+. However, three lines of evidence suggest that NPCs are not as wide as the canon of cell and molecular biology dictates (5, 6). Due to their importance in establishing the physiological significance of NICs, and therefore, that of the results presented here, a brief examination of these experimental observations is given below.

First, high resolution electron microscopy shows that NPCs contain a large restrictive central plug ($\sim$megadaltons; 7–10). In a yet more recent publication, the architecture of NPCs has been proposed to consist of a large central pore surrounded by eight smaller, equidistant pores (11). Thus, this recent observation opens the possibility that when the large central pore is plugged (e.g., when large molecules like RNA are not being transported) the peripheral, relatively tiny, channels may become the predominant causeways for the movement of ions across the NE. Furthermore, this massive plug may also play an important role in NIC gating and/or modulation when it does not completely obstruct the NPC (i.e., by reducing the effective pore diameter). Therefore, a structural foundation does exist for correlating NICs to NPCs.

Second, recent fluorescence microscopy of a variety of preparations (12–17) have confirmed previous cell biology findings (e.g., autoradiography) indicating that several ionic species are differentially distributed between nucleus and cytoplasm (18–21, reviewed in reference 3). This heterogeneous distribution of ions and molecules between the nucleosol and cytoplasm has been interpreted in terms of either a high or a low resistance to the flow of the particles investigated. For example, the concept that water exists in different states within cellular compartments, and in particular within the nucleus, has been used to explain the unequal distribution of ions coexisting with a highly porous, thus low electrical resistance, NE (18, see reference 3). This idea, like others emerging from the electronegativity of DNA molecules (e.g., Donnan effect), will be further explored in the next paragraph dealing with electrophysiological data. In contrast, a restrictive barrier to ion flow (high electrical resistance) at the level of the NE has been proposed on the basis of high-resolution confocal scanning fluorescence microscopy (utilizing ratiometric approaches that take care of probe compartmentalization by intracellular organelles) (13, 14). Similar divergent lines of interpretation may be given to the nucleocytoplasmic electrical potential detected with fluorescent probes (22, 23). Therefore, evidence other than electrophysiological suggests that the NE may function as a barrier to ion flow.

Third, patch-clamp measurements in a variety of animal and plant preparations show that flow of small physiological ions across the NE is highly resistive, in the order of gigaohms per square micrometer of NE surface area (1, 24–28). According to these studies, ion flow across the NE should be accomplished through NICs nec-

Symbols used: approximately ($\approx$); in the order of ($\sim$), i.e., closest numerical representation in base 10.

Abbreviations used in this paper: dNTP, deoxynucleotide; *i*, electrical current-dependent variable; NE, nuclear envelope; NIC, nuclear ion channel; NPC, nuclear pore complex; *t*, time-independent variable; TEA, tetraethylammonium; TEACl, tetraethylammonium chloride; TTX, tetrodotoxin; *V*, electrical potential or voltage-independent variable; V_{rev}, value of *V* at which *i* reverses direction.

0006-3495/93/06/1735/15 $2.00

essarily related to the NPCs since electron microscope observations revealed that several NPCs are contained under the patch-pipette (24, 25, 27; see recent discussion in reference 5, last paragraph of page 197 in reference 25, and evidence of three decades ago in reference 29). NICs are electrophysiologically (e.g., conductance parameters, open and closed states) and, to certain degree, structurally (e.g., expand over two membranes) similar to better-known gap junctional channels (30) but seem to have a much larger conductance than cell surface membrane ion channels (see discussion in references 24 and 25, see also reference 55). As patch-clamp data was obtained from isolated nuclei, it could be argued that the recorded high electrical resistance of the NE resulted from technical artifacts imposed by nuclei isolation and which led to closure of NPCs. That this is not the case was demonstrated three decades ago by Loewenstein's laboratory with microelectrodes inserted in situ in single nuclei of giant salivary gland cells (31, see also references 32–37). Under these conditions, the in situ NE was found to have an electrical resistance much higher than that predicted by tracer (radioactive and fluorescent) experiments (18–21, see reference 3). Furthermore, the in situ nucleus was shown to have a resting potential negative with respect to the cytoplasm. Experiments by another laboratory also found similar nuclear resting potential in a different preparation (38). Interestingly, these classical electrophysiological measurements of membrane potential and resistance demonstrated that the NE of oocytes (a preparation favored for electron microscopy analysis) offers less resistance to ion flow than the NE of salivary gland cells. However, these lower values of membrane potential and resistance in oocyte NEs have been taken to be a result of technical difficulties (i.e.), microelectrode damage of preparation; see, for example, footnote of page 321 in reference 3). Curiously, the proposed NE damage by the microelectrode was not used to explain why the resting electrical potential (recorded with salt-bridges, a must to measure Donnan potentials; see reference 39, seldom used in patch-clamp tests) disappears upon NE puncture (37), indicating a diffusional and not a Donnan potential. Clearly, the relatively high density of the nuclear material makes it difficult to give a simple interpretation of nuclear electrical phenomena in terms of say the Donnan effect (e.g., see page 82 in reference 39) or other electrical charge effects (40). That the NE is capable of transporting large particles is not at issue here. The NE may transport large molecules that contain proper "localization" signals (peptide sequences recognized by "receptors" at the NE). This transport is a mediated and/or regulated transport and requires energy (ATP hydrolysis, e.g., 41–45). Thus, classical and current electrophysiological data obtained in situ and in vitro speaks in favor of the existence of nuclear membranes (from various cell types) resistive to ion flow (with exceptions perhaps related to cell cycle and functional states; see, for example references 35 and 37). That transport of ions may be restricted and concomittant to transport of large molecules does not seem to be a exclusive property of the NE, for the cell surface membrane has similar types of transport systems. The difference is, however, that at the level of the NE this dual role seems to be played by the macromolecular structure of the NPC.

On the basis of the above evidence, one may reach the following conclusions. First, measurement of NIC electrical conductance provides an estimate of NE (thus NPC) permeability. Therefore, NIC conductance gives an index of nucleocytoplasmic transport (e.g., influx of cytosolic signals for regulatory reactions, and of nucleotides for nucleic acid polymerization) since each time the NPC gates open, ion flow must occur (unless the transported macromolecule fit tightly to the opening of the NPC). And second, NIC function (i.e., conductance properties such as opening and closing frequency and its modulation by voltage and chemical environment) is an important mechanism resulting from the integration of signals travelling to and from the nucleus (41–45), and determining the transfer of these signals across the NE. Indeed, cAMP-dependent protein kinase phosphorylation, known to increase nucleocytoplasmic transport and gene activity (42–45), was recently shown to stimulate cardiac NIC activity (1).

The present investigations extend previous observations on the sensitivity of cardiac myocyte NICs to cytosolic signals known to play important roles in signal transduction and gene-related processes (i.e., cAMP-dependent pathways; see reference 1). The cationic, K^+-dependent nature of NICs in cardiac myocytes was demonstrated in inside-out, excised patches, by the reduction in outward current following replacement of nucleoplasmic KCl with tetraethylammonium (TEA) chloride (TEACl) while maintaining cytoplasmic KCl. That Cl^- was not involved was demonstrated by the lack of effect of Cl^- replacement by aspartate or glutamate. The nuclear channels did not relate to conventional Na- or Ca-channels as 100 μM TTX and diltiazem did not alter NIC activity. Cardiac myocyte NICs were blocked by 100 μM cytoplasmic Zn^{2+}. The experiments show that NIC activity is reduced by GTP-dependent process(es), as shown by the inhibitory effects of the nonhydrolyzable GTP analog GTP-γ-S (10 μM), and increased by a mixture of 200 μM dNTPs. Thus, it appears that GTP-dependent processes play adversary roles to cAMP-dependent processes in regulating NIC activity. Therefore, assuming that NICs are physically related to NPCs, NICs may decide what goes in and out of the nucleus—a function that may be viewed as a mechanism controlling gene activity.

MATERIALS AND METHODS

Nuclei isolation

A simple technique requiring about 20 min processing, was developed following principles described elsewhere (1). Briefly, twelve male

Swiss-Webster mice (20–22 g, Charles River Labs./Bausch & Lomb Inc., Montréal, Québec) were utilized according to the Animal Care guidelines. The hearts were extracted, placed rapidly in a solution (mM: 150 NaCl, 2 $MgCl_2$, 5 Hepes and 2.5 KOH, room temperature: 22–24°C), and then cleaned of blood by 3-min retrograde perfusion as reported previously (46). A mixture of collagenase XI (500 U/ml, Sigma Chemical Co., St. Louis, MO) and protease XIV (1 U/ml, Sigma) was added to the perfusing solution for 1 min in order to digest the intercellular matrix (47). The digestive enzymes were cleaned off the heart by further 3-min perfusion with the enzyme-free solution supplemented with protease inhibitor (1,000 U/ml, Sigma). A cell suspension was prepared by cutting the softened ventricles and promoting cell disaggregation by 1-min magnetic stirring (46). The cell suspension was passed through a 100 μm nylon gauze as reported (48). A myocyte pellet was prepared by Percoll™ gradient (Pharmacia Fine Chemicals, Uppsala, Sweden). An initial suspension of $\sim 10^5$ cells/ml was centrifuged for 5 min at 34 *g* (room temperature). The pellet was washed twice in ice-cold solution (mM: 135 KCl, 2 $MgCl_2$, 5 EGTA, 5 Hepes and 17.5 KOH) and then placed in a 7-ml Dounce manual tissue grinder (Wheaton-33™ low extractable borosilicate glass; Wheaton, Millville, NJ) containing the ice-cold solution. After 3 min equilibration, pellet grinding proceeded with the loose-fitting pestle in 4–8 strokes. Nuclei isolation was monitored by a high-resolution light microscope (49). Myocyte homogenates containing the isolated nuclei were kept in the high-K, EGTA solution at 2–4°C for up to 4 h. The nuclei readily attached to the glass bottom of the 1-ml experimental chamber (46) and could be cleaned from debris by chamber perfusion.

Fluorescence microscopy

Nuclei were identified by their conspicuous morphology under light microscopy and their fluorescence at 520 nm excitation wavelength after 1 min treatment with 1 μg/ml of the DNA marker ethidium bromide (Sigma). Fluorescence microscopy was possible with a custom microscope (49) equipped with a 200 W stabilized arc lamp system (Photomax™, Oriel Corp., Stratford, CT) and with excitation and emission filters of 520 and 590 nm, respectively (Omega Optical Inc., Brattleboro, VT). Ethidium bromide-treated nuclei were not utilized in patch-clamp experiments.

Solutions

Salt solutions were prepared with AnalaR-grade reagents (BDH Chemicals Inc., Toronto, Ontario) and with Type I reagent grade water (≥18.2 MΩ · cm) obtained *'on demand'* from a water purification system (Milli-Q^{UF}-PLUS and 0.22 μm Millistak-GS filter, Millipore Corp., Bedford, MA). Solutions had a pH of 7.2–7.4 and a $pO_2 > 150$ mmHg. The solutions were freshly prepared in Teflon™ ware (Nalgene, Nalge Co., Rochester, NY) to minimize contamination. Pipettes were filled with freshly prepared solutions via Teflon™ syringes (Chromatographic Specialties Inc., Brockville, Ontario) and filters (Nalgene) to prevent contamination (e.g., 50). A lowering of pH with overnight storage of solutions in syringes, was detected and, therefore, avoided through the usage of fresh solutions. The control solution was a high-K-MgATP solution consisting of (mM): 150 KCl, 4 MgATP, 5 Hepes, 2.5 KOH. Hepes, TTX, MgATP, GTP-γ-S and deoxynucleotides (dNTPs: dATP, dCTP, dGTP, dTTP and dUTP) were purchased from Sigma. Solution exchange in the experimental chamber was estimated visually with dyes and electrically via measurements of electrode polarization. Complete exchange was achieved within 5 s. This time was taken into account when assessing the effects of different maneuvers on NIC activity. Temperature of solutions in the chamber was 36 ± 1°C (PE-2 water bath, Haake, Mess-Technik GmbH & Co., Karlsruhe, Germany; customized to eliminate electromagnetic interference). Chamber temperature was monitored with a thermistor (YSI 44004; Yellow Springs Instrument Co., Yellow Springs, OH) connected to a data acquisition system (51).

Patch-clamp

Standard patch-clamp techniques (52) were utilized throughout the investigations. Five mm-shank pipettes were made in a two-stage puller (PB-7 Narishige Co., Tokyo) from hard borosilicate glass (7052; Corning Glass Co., Corning, NY; capillaries of 0.5 mm-wall thickness, prepared by Garner Glass Co., Claremont, CA). Pipettes were heat-polished to an external diameter of 1–1.6 μm (0.2 μm resolution, see reference 49). The pipettes were electrically connected to the input headstage of a patch-clamp instrument (EPC-7, List Medical, Darmstadt/Eberstadt, Germany) and had a resistance of 4–6 MΩ. Mechanical stability was maximized by separating the pipette holder (EPC-7 accessory) from the input connector of the headstage and by firmly attaching it to the micromanipulator system. The micromanipulation system consisted of a piezo-electric translator block (0–100 μm per 0–1,000 volts: P-280.3-Physik Instrumente Gmbh & Co., Waldbronn, Germany) attached to a standard micromanipulator (Ernst Leitz Wetzlar Gmbh, Wetzlar, Germany). Experimental chamber and micromanipulators were mounted on a large microscope stage (49). The arrangement rested on a vibration-isolation table (Vibraplane 1201; Kinetic Systems, Inc., Roslindale, MA). Electrode polarization was compensated for and accepted as stable if the drift in polarization was less than 1 mV in 15 min (aided with overnight equilibration of the system with control solution and salt bridges made of Ag/AgCl half-cells: RC-2, World Precision Instruments, Inc., New Haven, CT, see reference 46). NE currents and potentials were measured, respectively, under the voltage- and zero-current clamp modes of the EPC-7 (see reference 1). Analogue signals were filtered at 1 kHz and amplified (CyberAmp Programmable Signal Conditioner equipped with an 8-pole Bessel filter, Axon Instruments, Foster City, CA) prior to digitization and storage by a fast data acquisition system (51). The signals were monitored on the screen of a standard oscilloscope (2225; Tektronix, Beaverton, OR) and stored on magnetic video tape (VR-10; Instrutech Corp., Elmont, NY) for off-line analysis. NIC activity was analyzed with custom (51) and commercial software (pClamp, Axon). The records shown in the figures were filtered at 100 Hz (pClamp). Filtering at this low frequency did not hide the essential properties of NIC conductance states and NIC reaction to the tests investigated in this study. Each experiment lasted between 0.5 and 1 h.

RESULTS

Morphological properties of isolated nuclei

Cardiac myocyte nuclei were readily identified by their ellipsoidal shape, morphological features such as nucleoli, their dimensions (see references 1, 48, 54), and their fluorescence when treated with ethidium bromide. Fig. 1 shows light microscope photographs aimed at illustrating the major characteristics of in situ and in vitro nuclei. Fig. 1 *a* gives a microphotograph of a piece of tissue after 2 strokes of the pestle in the tissue homogenizer. Only a few nuclei are obvious to the trained eye. Fig. 1 *b* illustrates the sample treated with ethidium bromide and under fluorescence microscopy. Under these conditions, not only nuclei are clearly seen by the untrained eye, but also their three-dimensional arrangement and individual perspectives. Fig. 1 *c* depicts isolated ventricular myocytes under conventional, dark-field illumination. Myocyte morphology is consistent with the general features of cardiac myocytes (46, 48). Fig. 1 *d* shows two isolated nuclei under fluorescence microscopy. In a previous study by this investigator (1) it was found that the major and minor geometrical axes of the nuclei were (mean ± SD): 13.6 ± 3.0 μm and

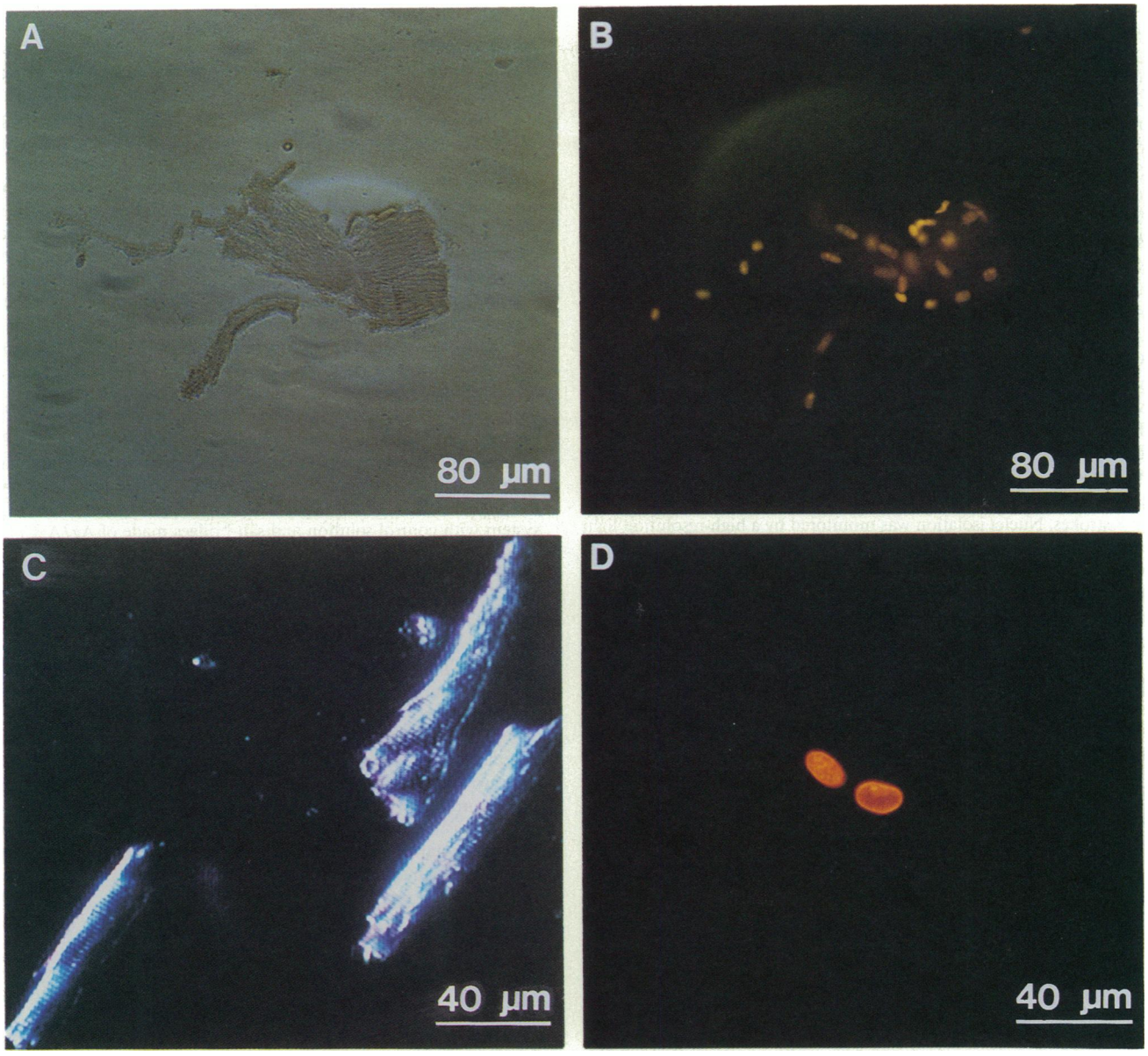

FIGURE 1 Morphological properties of cardiac myocyte nuclei as revealed by conventional light microscopy. (*A*) Photograph of a piece of ventricular tissue following 2 strokes of the pestle in the tissue homogenizer. No nuclei-associated feature is detected. (*B*) Photograph of the same sample treated with ethidium bromide and under conditions set for fluorescence microscopy. Not only nuclei are seen but also their three-dimensional arrangement and individual perspectives. (*C*) Isolated ventricular myocytes under conventional dark-field illumination show standard rod-shape features and striations. (*D*) Photograph of two isolated nuclei under fluorescence microscopy display typical ellipsoidal shape.

5.2 ± 1.1 μm, respectively ($n = 15$). The nuclei used here fall within these geometrical limits. NIC activity was observed in nuclei stored overnight at room temperature and in the myocyte homogenate. Data from these experiments are not included here but mentioned only to demonstrate the robustness of the preparation.

Cardiac myocyte NICs are cationic, with K^+ the major electrical charge carrier

Twenty experiments (one per patch) were conducted in excised, inside-out patches with the aim of identifying the ionic nature of the electrical charge carrier (four experiments for each TEACl, NH_4Cl, CsCl, K-aspartate, and K-glutamate). The high-K-MgATP solution was used as control for both the bath and pipette (see Materials and Methods). Only ions in the bath solutions were changed while maintaining MgATP. These experiments were carried out in inside-out patches to facilitate "bi-ionic conditions" under which only one major electrical charge carrier exist at each side of the membrane (see reference 55). The rationale behind this type of test has been discussed elsewhere (55) and is justified by the results obtained from this experimental series. Briefly, by

replacing only one ionic species at one side of the membrane one is able to determine its contribution to the net ion flow. Hence, if replacement of a particular ionic species does not affect the net current flow, that species is not involved. A shift in the reversal potential (V_{rev}, value at which the net current reverses its sign, or direction, with changes in transmembrane potential, thus indicating ionic equilibrium) provides a means of estimating the permeability ratio among the two ionic species tested (say X^+ and Y^+) according to the equation below (55):

$$V_{rev} = \frac{RT}{F} \ln \frac{P_X[X^+]_{cytosol}}{P_Y[Y^+]_{nucleoplasm}},$$

where R, T, and F have their universal meanings and $[X^+]_{cytosol}$ and $[Y^+]_{nucleoplasm}$ are the respective concentrations for X^+ and Y^+ at the outer (cytosolic- pipette solution) and inner (nucleoplasmic- bath solution) sides of the membrane under study (i.e., the NE). P_X and P_Y are the corresponding permeabilities for X^+ and Y^+.

Fig. 2 illustrates one of such experiments in which the bath KCl was replaced with an equimolar amount of TEACl. The current signals ($i(t)$) shown at the left column of Fig. 2 were elicited every 60 s with 10-s voltage ramps from +40 to −40 mV of transmembrane potential. During the 50 s between voltage ramps, the patch was held at 0 mV. Note that in inside-out excised patches the transmembrane potential is negative to the electrical potential applied to the pipette electrode. Also note that the $i(t)$ signals elicited with voltage ramps are equivalent to i vs. V plots (given the proper time-to-voltage transformation). Therefore, changes in the slope of these signals give an indication of how much the membrane conductance (an index of permeability) has changed. That is, slope increases reflect conductance increases and vice versa. Positive $i(t)$ signals represent outward movement (from nucleosol to cytoplasm) of positive charges (e.g., K^+) or inward movement (from cytosol to nucleosol) of negative charges (e.g., Cl^-). Note that in these experiments where inside-out excised patches were used, both types of charge movements are caused by negative pipette potentials. The opposite applies to negative signals. The horizontal dotted line drawn at the $i(t) = 0$ pA level corresponds to the value of $i(t)$ when no voltage was applied to the NE. Under control conditions (equal concentrations of the electrical charge carrier since same solution was used in bath and pipette) $i(t)$ reversed sign when the ramp potential reversed sign (i.e., $V_{rev} = 0$ mV, see reference 1). The plots on the right column of Fig. 2 were obtained after dividing the current signals, $i(t)$, by the corresponding, programmed voltage waveform ($V(t)$, the negative of the pipette potential in excised patches). Note that this mathematical transformation (i.e., $i(t)/V(t)$ frequently led to a large artifact near null potentials as a result of the division by minute numbers. (Manipulations during the mathematical analysis of recent experiments have shown that this artifact may be removed by forcing a small baseline value of a few mV on the voltage signals. Thus, it is likely that these errors emerge from minute potentials at the output of the digital-to-analogue converter utilized to generate the voltage-clamping waveform.) Therefore, the $i(t)$ vs. V plots on the right of Fig. 2 give the direct values of membrane conductance as a function of applied voltage. Membrane patches containing multiple ion channels (but not enough as to obscure occasional single-channel features) will display both microscopic (single-channel) and macroscopic (multi-channel, but not necessarily average) behavior. Hence, from these multi-channel experiments it was possible to determine whether ion movement was impaired by the ionic species replacement. Under control conditions, five top-left records, a linear, and otherwise featureless activity was observed. However, upon iso-osmolar (isotonic) replacement of K^+ by TEA^+ in the bath, five lower-left records, inward rectification developed. That is, it became harder for TEA^+ to move outwardly across the membrane. This change was concomittant to a shift in the reversal potential, V_{rev}, of $+51 \pm 8$ mV (mean ± SD, $n = 4$) from the control value of 0 mV. This phenomenon can be taken to mean that the permeability ratio for K^+ over TEA^+ ≈ 7.4, as per above equation for bi-ionic conditions. The TEA-induced effects were reversible upon return to control conditions (not shown). Note that the usage of a few records, rather than one, to represent control and test conditions is preferable due to the stochastic nature of the NIC activity studied (53). In eight experiments, replacement of bath KCl with CsCl or NH_4Cl did not produce a measurable change in either V_{rev} or NIC opening characteristics (not shown). Eight additional experiments in which bath chloride ions were replaced with aspartate or glutamate ions showed that chloride ions did not contribute to the net current flow (not shown). Taken together, these results strongly indicate that although NICs are not very selective among several cations (e.g., K^+, Cs^+, and NH_4^+), under normal conditions K^+ (and not Cl^-) ions are the major electrical charge carriers for NIC currents.

Cardiac myocyte NICs are insensitive to the channel blockers tetrodotoxin and diltiazem

It has been proposed that, upon their synthesis, ion channels-in-transit may move through cytosolic organelles (56). Therefore, experiments were carried out with attached and inside-out, excised patches in the presence and absence of the Na-channel blocker TTX (four experiments) and the Ca-channel blocker diltiazem (four experiments) at either side of the NE (note that since the NE consists of two membranes, it was deemed necessary to test both sides for potential binding sites, see reference 55). Fig. 3 depicts the results of one of these experiments which demonstrates the apparent lack of change in NIC activity when 100 μM TTX was added to the control, high-K-MgATP solution in the bath. In these experi-

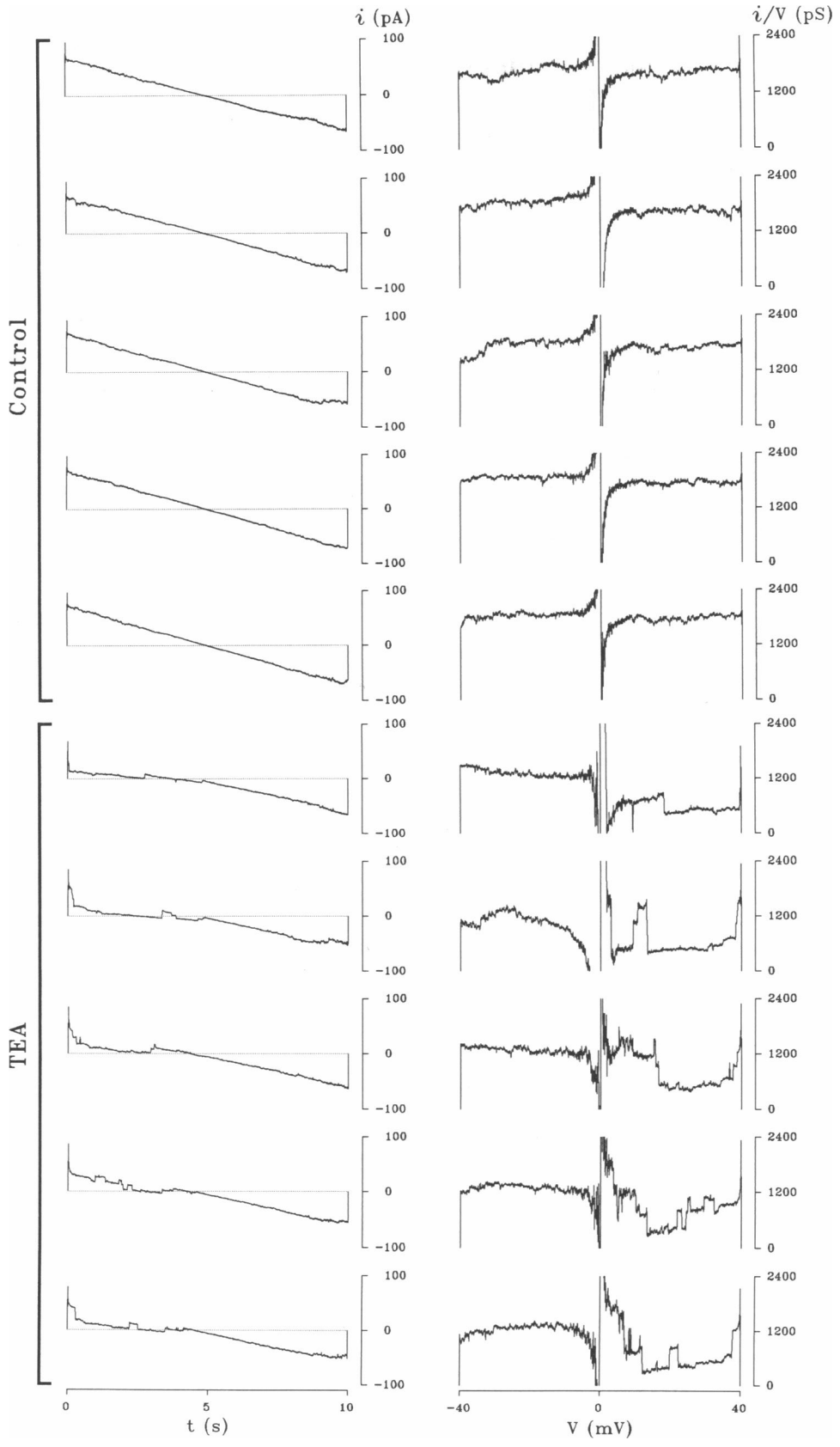

FIGURE 2 Cationic nature of cardiac myocyte NICs. (*Left*) Current signals $i(t)$ recorded while applying 10-s voltage ramps from +40 to −40 mV at 60 s intervals. The pipette potential was set to 0 mV during the period between consecutive voltage ramps. Positive signals represent movement of positive charges from nucleosol to cytosol or opposite movement of negative charges. The converse applies to negative signals. The horizontal dotted line drawn at $i((t) = 0$ pA shows the level of current when no potential (V) was applied to the patch. (*Right*) Plots of computed patch conductance (i/V) versus V. The small errors around $V = 0$ mV caused artifactual deviations in the calculated conductance as a result of the division of current records by very small numbers (i.e., this type of computation put a more stringent constraint in the measurement errors). Experiment carried out in an excised, inside-out patch at 35°C with high-K-MgATP solution. Bath KCl (150 mM) was replaced with TEACl (150 mM).

ments, voltage ramps were applied in a manner similar to that explained in the previous paragraph (describing tests for the determination of the major electrical charge carrier). Direct assessment of TTX action on NIC conductance can be accomplished from the computed conductance (i/V) versus potential plots on the right. No

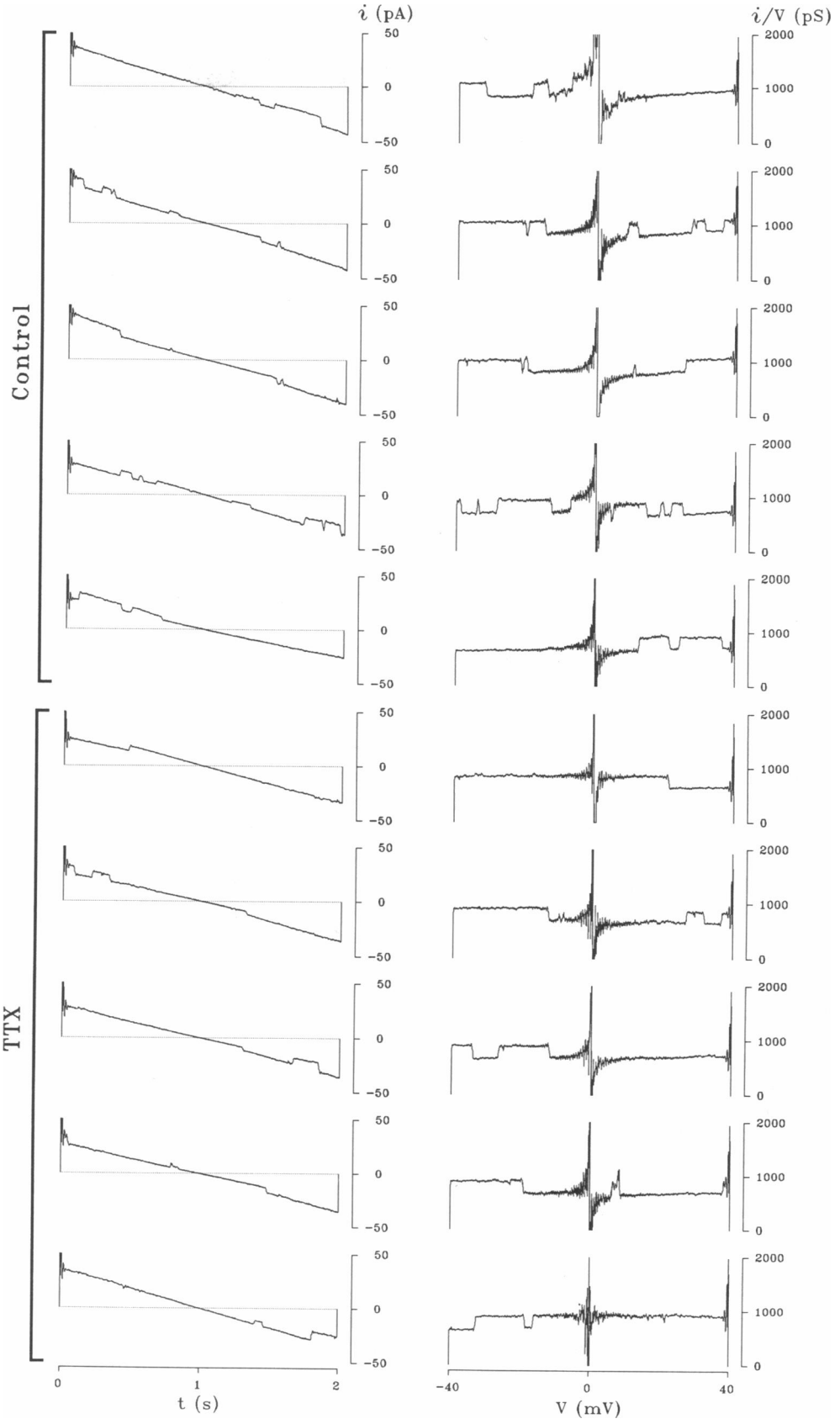

FIGURE 3 Effects of 100 μM of Na-channel blocker tetrodotoxin, TTX, on ventricular cardiac myocyte NICs. (*Left*) Current signals $i(t)$ recorded while applying 2-s voltage ramps from +40 to −40 mV at 30 s intervals. The pipette potential was held at 0 mV between ramps. (*Right*) i/V versus V plots. Experiment carried out with a nucleus-attached patch at 37°C with the high-K-MgATP solution. The control solution in the experimental chamber was replaced by the same containing TTX.

effects (shift in reversal potential or changes in average slope or single-channel conductance) were seen when the pipette was filled with control solution and backfilled (for a detailed description of the backfilling method, see reference 57) with TTX (two of the four patches) or when the nuclei were pretreated with the toxin (two additional patches). It should be noted that with the backfilling method there is no possibility of returning back to the control solution (i.e., washout of test substance is impossible). The results from similar tests with 100 μM diltiazem were also negative (not shown).

Cardiac myocyte NICs are blocked by Zn^{2+}

Since many nuclear components contain putative zinc-finger motifs (58) and Zn^{2+}-dependent reactants (59–60), four tests were conducted with voltage ramps (see paragraph on tests for determination of major electrical charge carrier) in attached and excised patches with 100 μM Zn^{2+} for the purpose of relating the effects of this important ion species to NIC activity. As Fig. 4 shows, NIC activity in a nucleus-attached patch was completely suppressed (i.e., reduction in the slope of $i(t)$ signals during the voltage ramps) when Zn^{2+} was added to the perfusate, an effect that was obviously indirect and mediated through intranuclear pathways. Zn^{2+} also blocked NICs when the pipette filled with control solution was backfilled with Zn^{2+} (two tests). Changes in reversal potential, V_{rev}, were undetectable. Thus, Zn^{2+} effects on NIC activity seem to be both direct and indirect. Similarly, Cd^{2+}, Co^{2+}, and La^{3+} were tested in six additional patches (two patches for each substance) and found to be blockers of NIC activity at similar concentrations (not shown), indicating that Zn^{2+} is not a useful marker or ligand for NICs.

Cardiac myocyte NICs are depressed by GTP-γ-S

GTP hydrolysis has been shown to affect nucleocytoplasmic transport (61). Therefore, four tests with 10 μM of the non-hydrolyzable GTP analogue GTP-γ-S were conducted to test this possibility. The tests were conducted with voltage ramps in a manner similar to that described for Figs. 2–4. Fig. 5 illustrates the depressing effect of GTP-γ-S on NE conducting properties in a nucleus-attached patch. As the effects were observed in nucleus-attached patches, it becomes evident that intranuclear molecules mediated the phenomenon. In two experiments with GTP-γ-S-backfilled pipettes, similar negative regulation of NIC activity occurred, indicating a less convoluted pathway for the action of this substance on NIC opening. That is, there must exist GTP-binding sites susceptible to hydrolysis at the membrane side facing the cytosol and, in addition, a site facing the nucleosol or within the nuclear material. However, the results were inconclusive when the GTP analog was directly applied to the nucleoplasmic side of excised, inside-out patches (two tests stimulated and two depressed NIC activity). This may be taken as an indication that other components needed for the effects of GTP-γ-S were not always present in the tests. GTP did not have a measurable effect in either excised or attached patches (not shown). Therefore, these results suggest an important role for GTP hydrolysis in NIC function.

Cardiac myocyte NICs are stimulated by deoxynucleotides

Six tests with 200 μM dNTPs demonstrated that an increase in cytosolic dNTPs may trigger NIC activity. Fig. 6 shows the results of one of these experiments in a nucleus-attached patch. Voltage protocols were as in Figs. 2–5. The records shown for control and test-dNTPs conditions were consecutive as the nature of NIC activation was transient. It is not clear whether the phenomenon is use-dependent (i.e., if it was dependent on the rate at which the pulses were delivered) for this possibility was not tested. In other words, the observation of a transient increase in NIC activity may indicate a repriming interval (e.g., for an enzyme pool) being needed before NIC opening through dNTPs stimulation. No measurable effects were observed in three excised patches when the control solution in the bath was replaced by the same containing dNTPs or when the recording patch-pipette was backfilled with the dNTPs (three patches). This suggests that the transient NIC stimulation by dNTPs occurs only through indirect, nuclear-delimited, pathways.

DISCUSSION

Morphological properties of cardiac myocyte nuclei

Cardiac myocyte nuclei were isolated within 20 min by utilizing a method that shortcuts standard cell and molecular biology procedures. The principle behind the method was to reduce potential deleterious effects on nuclear integrity, with special attention paid to the NE and the NPCs. Hypotonic and/or detergent treatment-common to standard cell and molecular biology isolation methods- were avoided since such treatments have been correlated to removal of the large central plug from the NPCs (9). The fact that the isolated nuclei remained functional for more than 24 h when stored overnight in the cell homogenate, and at room temperature, shows not only the robustness of the preparation but also the important role of cytoplasmic factors in NE, NPC and NIC integrity (62, 63). This resilience of the isolated nuclei may be exploited in future investigations and is especially relevant if lower storage temperatures can be employed. As shown in Fig. 1, the nuclear morphology is quite agreeable with the light microscopy observations made routinely by this (1, 48) and other laboratories (54). The large size of cardiac myocyte nuclei should

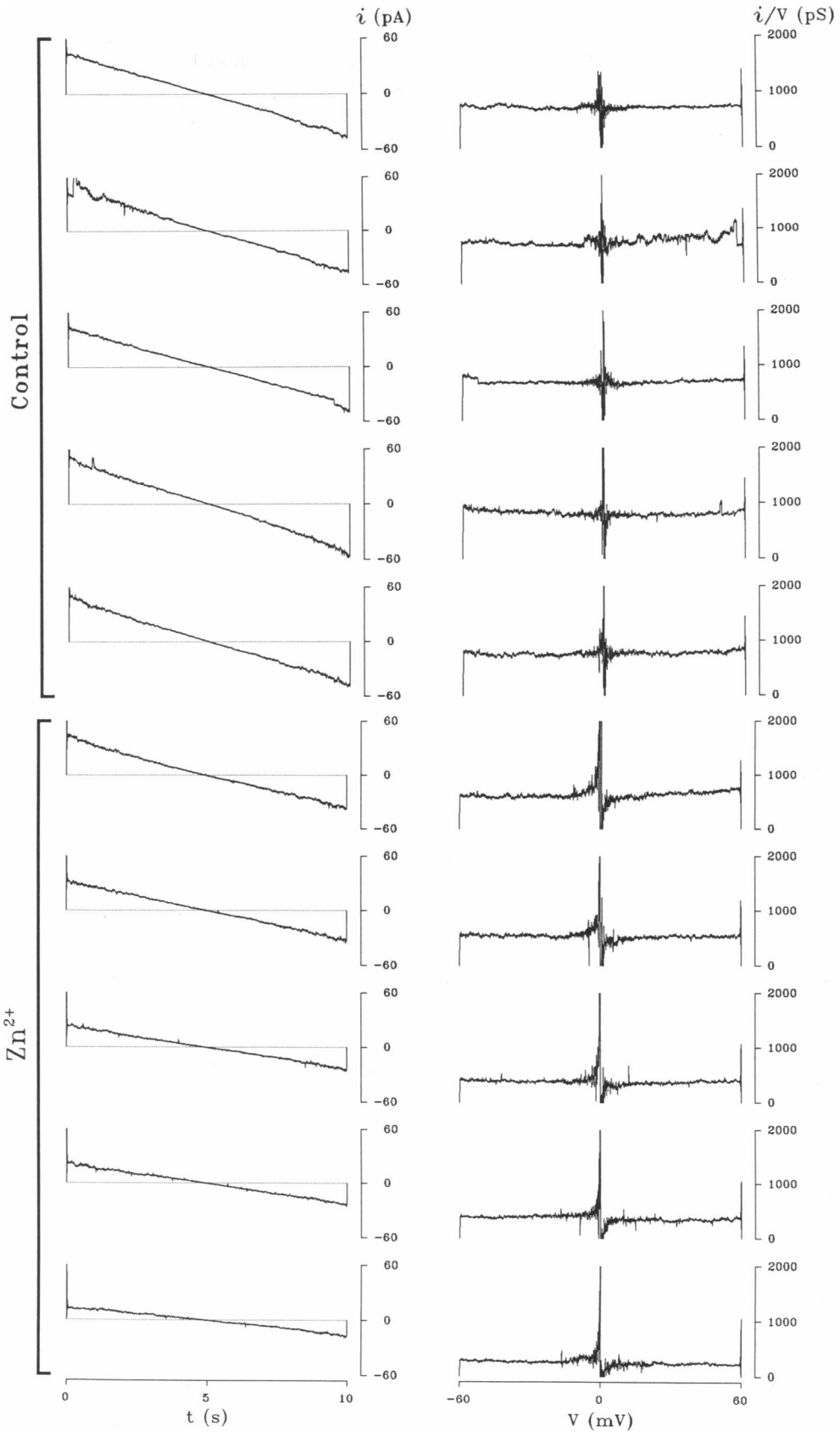

FIGURE 4 Effects of 100 μM Zn^{2+} on ventricular cardiac myocyte NICs. (*Left*) Current signals $i(t)$ recorded while applying 10-s voltage ramps from +60 to −60 mV at 30 s intervals. Pipette potential was set to 0 mV between ramps. (*Right*) i/V versus V plots. Experiment carried out with a nucleus-attached patch at 37°C with the high-K-MgATP solution in bath and pipette. A $ZnCl_2$-containing solution replaced the control solution in the experimental chamber.

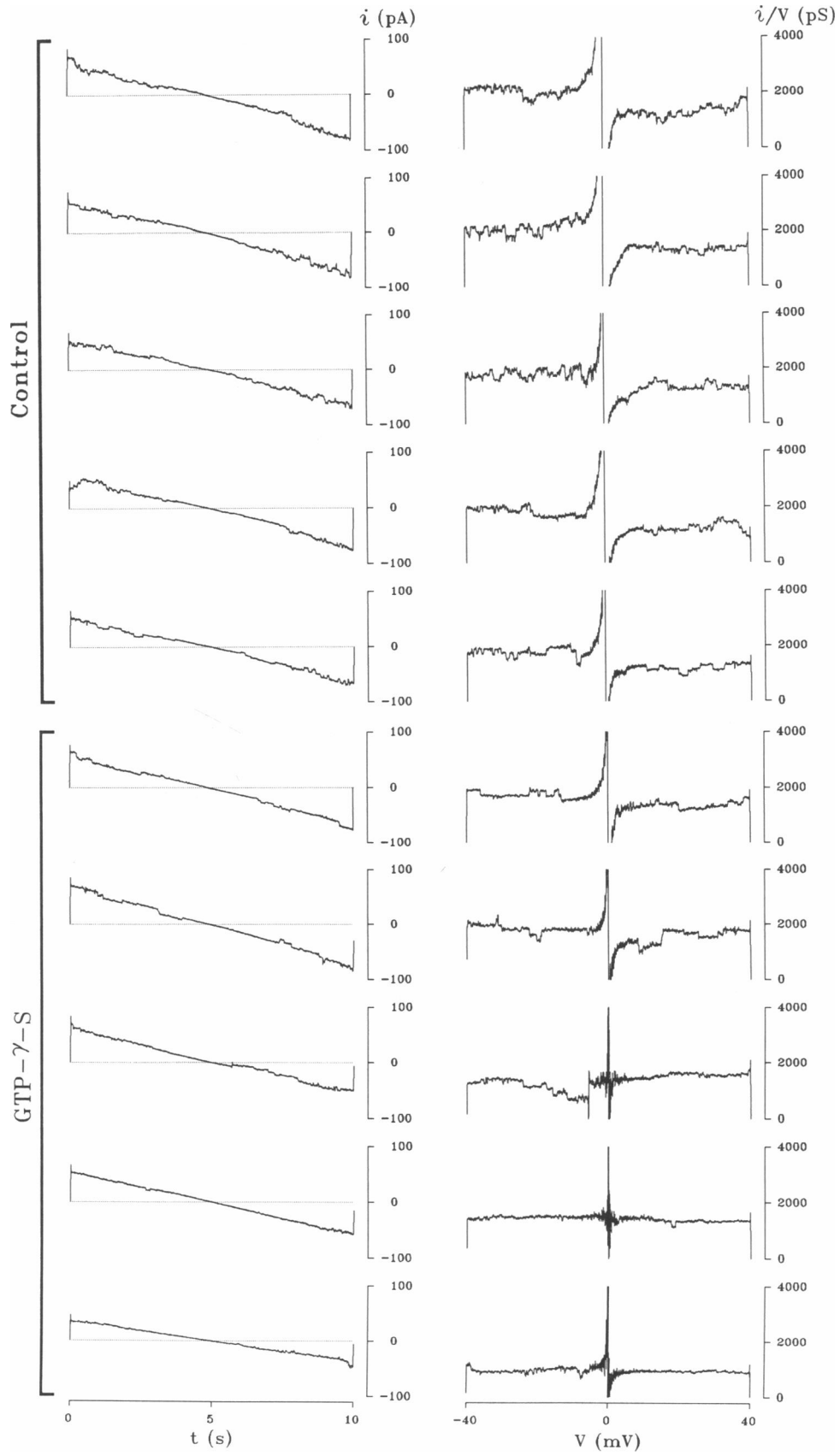

FIGURE 5 Effects of 10 μM non-hydrolysable GTP-γ-S on ventricular cardiac myocyte NICs. (*Left*) Current signals $i(t)$ recorded while applying 10-s voltage ramps from +40 to −40 mV at 60 s intervals. The pipette potential was held at 0 mV between the voltage ramps. (*Right*) i/V versus V plots. Experiment carried out with a nucleus-attached patch at 35°C with the high-K-MgATP solution in bath and pipette. The control solution in the experimental chamber (bathing the cytoplasmic side of the nucleus) was replaced by the same containing GTP-γ-S.

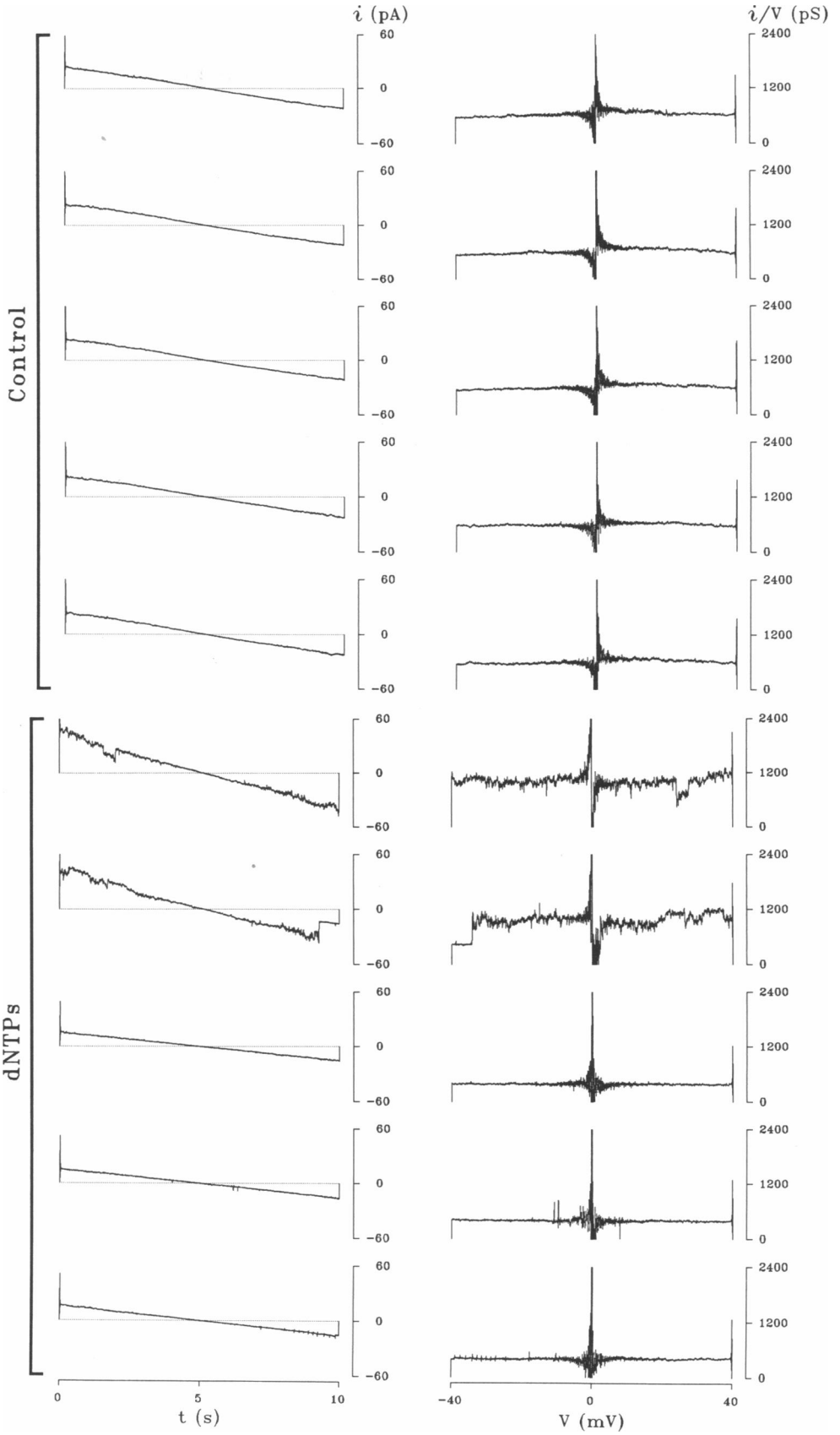

FIGURE 6 Stimulation of cardiac myocyte NIC activity by 200 μM cytosolic dNTPs. (*Left*) Consecutive current signals $i(t)$ recorded while applying 10-s voltage ramps from +40 to −40 mV at 60 s intervals. The pipette voltage was set to 0 mV between the ramps. (*Right*) i/V versus V plots. Experiment carried out with a nucleus-attached patch at 35°C with the high-K-MgATP solution in bath and pipette. The control solution in the experimental chamber was replaced by the same containing dNTPs.

make them a suitable preparation for future studies. As pointed out previously (1), isolated nuclei appear at times with endoplasmic reticulum remains. The nuclei selected for the present studies were devoid of such remains. The fact that the isolated nuclei attached firmly to the glass bottom of the experimental chamber, aided in washing away homogenate debris from the nuclei.

Cardiac myocyte NICs are cationic with K^+ the major electrical charge carrier

That under normal physiological conditions K^+ is the major electrical charge carrier through cardiac myocyte NICs was revealed by the tests in which cationic and anionic species substitution took place. These tests were conducted in excised, inside-out patches since under these conditions there is a good control of the solutions bathing both sides of the patch, thus allowing the direct assessment of permeability ratios from the shifts in reversal potential, V_{rev}. The apparently passive, linear (as a function of voltage) and otherwise featureless NE conductance (e.g., control panel in Fig. 2) was revealed to result from the opening of several NICs when K^+ was replaced by a relatively impermeant cation such as TEA^+ (e.g., TEA panel in Fig. 2). TEA^+ (in the form of TEACl) was selected as the best example because pH and tonicity were not altered by this replacement in the ion species (as it occurred with other large cations). Interestingly, the experiments with Cs^+ and NH_4^+ consistently yielded no measurable shift in V_{rev} and no change in NIC conductance, suggesting that NICs are geometrically large enough to allow passage ions as large as NH_4^+ and/or have a selectivity filter that does not distinguish between K^+, Cs^+ and NH_4^+ (i.e., large effective NIC radius, see reference 55). These results are in sharp contrast with the decrease of NIC conductance and activity upon exposure to Na^+ recently reported (1). Furthermore, the tests in which Cl^- was replaced with aspartate and glutamate anions demonstrated a negligible contribution of Cl^- to the normal activity of cardiac myocyte NICs under the present experimental model. It is not clear whether the ionic species tested have any effect on genetic processes and, as a result, whether genetic activity would have a feedback action on NIC function, due to the relatively short duration of the experiments (i.e., from the genetic point of view). The results indicate, therefore, that cardiac myocyte NICs could be classified within the large family of K-channels. Whether these channels relate to other known cardiac channels is discussed below.

Cardiac myocyte NICs are insensitive to the channel blockers tetrodotoxin and diltiazem

The tests with TTX and diltiazem were conducted to make certain that Na- and Ca-channels, in transit to the cell surface membrane, were not included in this preparation (see reference 56). As the experimental results showed (e.g., Fig. 3), cardiac myocyte NICs were insensitive to these channel blockers. Therefore, one could generalize that it seems unlikely that the NE was contaminated with ion channels in transit. Previous experiments by this investigator (1) and those presented here demonstrate that, under putative normal physiological conditions, NICs should favor the conduction of K^+ over that of any other physiological cation (including Na^+, see reference 1). As several K-channels are known to exist in cardiac myocytes, tests with K-channel blockers were deferred for future experiments. However, it is worth mentioning that the properties of cardiac myocyte NICs are somewhat different from those of several known cardiac sarcolemmal K-channels (55). For example, since NICs are functional in the presence of ATP it is unlikely that they are related to K-ATP channels since the latter are inhibited in the presence of ATP. Further, these K^+-conducting NICs were not affected by the presence (1) or absence of Ca^{2+} (5 mM EGTA; Bustamante, unpublished data), consequently, they do not seem connected to Ca^{2+}-activated K-channels. The lack of effect on NICs caused by K^+ replacement with Cs^+ and NH^{4+}, as well as the inability of TEA^+ to block these channels, suggests little relation with the delayed rectifying K-channel. Chloride NICs have been identified in rat hepatocyte nuclei on the basis of their response to Cl-channel blockers (28). In the present studies, NICs did not respond to Cl-replacement as discussed in the previous paragraph. Therefore, it was concluded that Cl^- played no role as charge carriers in cardiac NICs and that this lack of effect of anion species substitution precluded any rationale to justify tests with Cl-channel blockers.

Cardiac myocyte NICs are blocked by Zn^{2+}

It is known that Zn^{2+} is an important ion for the structure and function of genes (58, 60), RNA polymerases and transcription factors (59), etc. Consequently, the effect of Zn^{2+} on NIC activity was tested. The finding that 100 μM Zn^{2+} blocks or negatively modulates NIC activity (i.e., reduction of the slope of $i(t)$ signals elicited with voltage ramps, see Fig. 4) may be of relevance although it is difficult to ascertain at this moment a precise mechanism or purpose for the modulation of NICs by this cationic species. The effect was observed in nucleus-attached patches when the control bath perfusate was changed with the same solution but containing Zn^{2+} as well as when the pipette was backfilled. The high seal resistance, imperative of patch-clamp experiments (including the present ones), insures that there is virtually no mixing of bath and pipette solutions (52, 53). Therefore, the effects observed upon switching bath solutions (while having no change in the pipette solution) must have been indirect and mediated through the nuclear compartment. Likewise, the effects observed when the

pipette was backfilled with the test substance must have been a result of the actions of the test substance on the surface area covered by the pipette alone (i.e., no intranuclear mediation). The fact that Cd^{2+}, Co^{2+} and La^{3+} also blocked NIC activity suggest that Zn^{2+} is not a good marker for cardiac myocyte NICs. Taken together the results from the tests with ionic species substitution, and from those utilizing organic and inorganic Na-, Ca- and K-channel blockers (present and previous paragraphs) it would seem that NICs are a distinct class of K-channels intrinsic to the nuclear membrane and part of the NPC. Future work with cell and molecular biology techniques should clarify this point (e.g., by usage of antibodies specific to NPC components).

Cardiac myocyte NICs are depressed by GTP-γ-S

An interesting finding was that of NIC depression by GTP-γ-S (see Fig. 5) and not GTP. This result indicates that when bound to a particular molecule site in the NE (likely to be a candidate GTP-binding protein), hydrolysis of GTP follows. However, should the GTP hydrolysis be impaired or negatively modified, then, NICs would tend to remain in the closed, nonconducting state. How this experimental observation relates to the GTP-γ-S-induced inhibition of vesicle fusion during NE assembly (61) is not clear but the present experiments provide a basis to speculate that GTP hydrolysis is involved in NIC function. The GTP-mediated closure of NICs may be a mechanism involved in cell transformation (see reference 64 and references therein). The fact that experiments where GTP-γ-S was applied directly to the intranuclear side of the patch (i.e., inside-out, excised patches, with the GTP analogue applied to the bath solution) did not yield conclusive results (two tests gave positive and two gave negative results) suggests not only more experiments are needed but also that components yet to be determined may mediate the action of this substance. Clearly, since effects were recorded in nucleus-attached patches, intranuclear mechanisms mediate the action of GTP-γ-S. Depression of NIC activity was also observed when GTP-γ-S backfilled a pipette filled with control solution. This shows that GTP may also act directly from the cytosolic side of the NE.

Cardiac myocyte NICs are stimulated by deoxynucleotides

dNTPs are the raw material required for the synthesis of deoxyribonucleic acids (4). Therefore, cytosolic dNTPs must reach DNA templates by crossing the NPCs (4), which are assumed here to be the physical substrate of NICs (see also references 1, 24, 25). The experimental results presented here (e.g., Fig. 6) demonstrate that although dNTPs (in a MgATP-containing solution) may be sufficient to trigger NIC openings, other nuclear substrates such as kinases or polymerases may be required for sustained NIC activity; otherwise, the stimulation is only transient, short-lived. The effects of dNTPs on NIC activity, however, may have been a result of mere allosteric interactions (e.g., 65). Although experiments recently carried out by this investigator (Bustamante, unpublished data) with AMPP(NH)P-Mg^{2+} replacing MgATP (to minimize phosphoryl donation by ATP) did not substantiate such possibility, a full screening of the allosteric effects of dNTPs is required to make a qualified exclusion of this mechanism. As dNTPs were only effective when acting through intranuclear-delimited pathways, this may indicate that dNTPs trigger some sort of reaction in the intranuclear space (perhaps a genetic one such as activation of transcription) which, in turn, transfer the request for NIC opening from the nucleoplasmic side of the NE. This rather complex reaction falls within the variability of conductance states seen for cardiac myocyte NICs (1).

Potential role of NICs in mediating transfer of matter and information to and from the genetic machinery

The present work shows for the first time the modulation of cardiac myocyte NICs by GTP-associated processes, dNTPs, and Zn^{2+}. The fact that NPCs are thought to be solely responsible for nucleocytoplasmic transport (5, 6, 20, 41, 43), along with the current and previous observations on NIC activity (1, 24–28), suggests a physical correlate between NPCs and NICs. This is reinforced by the demonstration with electron microscopy that NE patches contain several NPCs (25, 27). The rather complex structure of the NPCs (7–11) as well as their associated environment (4–6, 41–45) is suggestive of a multilateral control of NIC activity: both from within and from without the nucleus. As nucleocytoplasmic ion distributions seem to be important in the control of nuclear processes (e.g., transcription and other DNA-related activities, see references in 3, pages 319–320), NICs should play a major role in the determination of normal and pathological states of cell structure (e.g., growth and hypertrophy) and function (e.g., normal and impaired secretion). The potential significance of NIC studies (i.e., present studies and references 1, 24–28) stresses the importance of elucidating the molecular identify of these ion channels. Most important seems to be the clarification of the apparent conflict of these studies with those suggesting unrestricted flow of ions across the NE (3). For this purpose, the use of antibodies (to specific molecules of NPCs) in patch-clamp experiments would seem the next logical step.

The author tenders his gratitude to his colleagues Drs. Stuart L. Jacobson, Mike McBurney and Eef Harmsen for constant helpful discussions and to Drs. Michele Mazzanti, Louis J. DeFelice, Bertil Hille, Sandy Simon, Christopher W. Akey, Colin Dingwall, and Larry Gerace for short but effective constructive comments.

This work was possible thanks to the generous support of the New Brunswick Heart and Stroke Foundation and the University of Ottawa Heart Institute (at which the work was carried out).

Received for publication 15 September 1992 and in final form 12 January 1993.

REFERENCES

1. Bustamante, J. O. 1992. Nuclear ion channels in cardiac myocytes. *Pflügers Arch.* 421:473–485.
2. Dingwall, C. 1990. Plugging the nuclear pore. *Nature* (*Lond.*). 346:512–514.
3. Paine, P. L., and S. B. Horowitz. 1980. The movement of material between nucleus and cytoplasm. *Cell Biol.* 4:299–338.
4. Alberts, B., D. Bray, J. Lewis, M. Raff, K. Roberts, and J. D. Watson. 1989. The cell nucleus. *In* Molecular Biology of the Cell. Alberts, B., D. Bray, J. Lewis, M. Raff, K. Roberts, and J. D. Watson, editors. Garland Publishing Co., New York. 481–549.
5. Dingwall, C. 1991. Transport across the nuclear envelope: enigmas and explanations. *BioEssays.* 13:213–218.
6. Hanover, J. A. 1992. The nuclear pore: at the crossroads. *FASEB* (*Fed. Am. Soc. Exp. Biol.*) *J.* 6:2288–2295.
7. Akey, C. W. 1991. Probing the structure and function of the nuclear pore complex. *Semin. Cell Biol.* 2:167–177.
8. Akey, C. W. 1992. The nuclear pore complex. *Curr. Opin. Struct. Biol.* 2:258–263.
9. Reichelt, R., A. Holzenburg, E. L. Buhle, Jr., M. Jarnik, A. Engel, and U. Aebi. 1990. Correlation between structure and mass distribution of the nuclear pore complex and of distinct pore complex components. *J. Cell Biol.* 110:883–894.
10. Jarnik, M., and U. Aebi. 1991. Toward a more complete 3-D structure of the nuclear pore complex. *J. Struct. Biol.* 107:291–308.
11. Hinshaw, J. E., B. O. Carragher, and R. A. Milligan. 1992. Architecture and design of the nuclear pore complex. *Cell.* 69:1133–1141.
12. Williams, D. A., K. E. Fogarty, R. Y. Tsien, and F. S. Fay. 1985. Calcium gradients in single smooth muscle cells revealed by the digital imaging microscope using Fura-2. *Nature* (*Lond.*). 318:558–561.
13. Hernández-Cruz, A., F. Sala, and P. R. Adams. 1990. Subcellular calcium transients visualized by confocal microscopy in a voltage-clamped vertebrate neuron. *Science* (*Wash. DC*). 247:858–862.
14. Hernández-Cruz, A., F. Sala, and J. A. Connor. 1991. Stimulus-induced nuclear Ca^{2+} signals in fura-2-loaded amphibian neurons. *Ann. NY. Acad. Sci. USA* 635:416–420.
15. Takamatsu, T., and W. G. Wier. 1990. High temporal resolution video imaging of intracellular calcium. *Cell Calcium.* 11:111–120.
16. Przywara, D. A., S. V. Bhave, A. Bhave, T. D. Wakade, and A. R. Wakade. 1991. Stimulated rise in neuronal calcium is faster and greater in the nucleus than in the cytosol. *FASEB* (*Fed. Am. Soc. Exp. Biol.*) *J.* 5:217–222.
17. Waybill, M. M., R. V. Yelamarty, Y. Zhang, R. C. Scaduto Jr., K. F. LaNoue, C.-J. Hsu, B. C. Smith, D. L. Tilloston, F. T. S. Yu, and J. Y. Cheung. 1991. Nuclear calcium transients in cultured rat hepatocytes. *Am. J. Physiol.* 261:E49–E57.
18. Century, T. J., I. R. Fenichel, and S. B. Horowitz. 1970. The concentrations of water, sodium and potassium in the nucleus and cytoplasm of amphibian oocytes. *J. Cell Sci.* 7:5–13.
19. Paine, P. L. 1975. Nucleocytoplasmic movement of fluorescent tracers microinjected into living salivary gland cells. *J. Cell Biol.* 66:652–657.
20. Paine, P. L., L. C. Moore, and S. B. Horowitz. 1975. Nuclear envelope permeability. *Nature* (*Lond.*). 254:109–114.
21. Horowitz, S. B., and P. L. Paine. 1976. Cytoplasmic exclusion as a basis for asymmetric nucleocytoplasmic solute distributions. *Nature* (*Lond.*). 260:151–153.
22. Matzke, M. A., and A. J. M. Matzke. 1986. Visualization of mictochondria and nuclei in living plant cells by the use of a potential-sensitive fluorescent dye. *Plant Cell Environm.* 9:73–77.
23. Matzke, M. A., A. J. M. Matzke, and G. Neuhaus. 1988. Cell age-related differences in the interaction of a potential-sensitive fluorescent dye with nuclear envelopes of *Acetabularia mediterranea*. *Plant Cell Environm.* 11:157–163.
24. Mazzanti, M., L. J. DeFelice, J. Cohen, and H. Malter. 1990. Ion channels in the nuclear envelope. *Nature Lond.)*. 343:764–767.
25. Mazzanti, M., L. J. DeFelice, and E. F. Smith. 1991. Ion channels in murine nuclei during early developments and in fully differentiated adult cells. *J. Membr. Biol.* 121:189–198.
26. Matzke, A. J. M., T. M. Weiger, and M. A. Matzke. 1990. Detection of a large cation-selective channel in nuclear envelopes of avian erythrocytes. *FEBS* (*Fed. Eur. Biochem. Soc.*) *Lett.* 271:161–164.
27. Matzke, A. J. M., C. Behensky, T. Weiger, and M. A. Matzke. 1992. A large conductance ion channel in the nuclear envelope of a higher plant cell. *FEBS* (*Fed. Eur. Biochem. Soc.*) *Lett.* 302:81–85.
28. Tabares, L., M. Mazzanti, and D. E. Clapham. 1991. Chloride channels in the nuclear membrane. *J. Membr. Biol.* 123:49–54.
29. Wiener, J., D. Spiro, and W. R. Loewenstein. 1965. Ultrastructure and permeability of nuclear membranes. *J. Cell Biol.* 27:107–117.
30. Peracchia, C. 1991. Biophysics of Gap Junction Channels. CRC Press, Boca Raton. 401 pp.
31. Loewenstein, W. R., and Y. Kanno. 1962. Some electrical properties of the membrane of a cell nucleus. *Nature* (*Lond.*). 195:462–464.
32. Loewenstein, W. R., and Y. Kanno. 1963. The electrical conductance and potential across the membrane of some cell nuclei. *J. Cell Biol.* 16:421–425.
33. Kanno, Y., and W. R. Loewenstein. 1963. A study of the nucleus and cell membranes of oocytes with an intra-cellular electrode. *Exp. Cell Res.* 31:149–166.
34. Loewenstein, W. R. 1964. Permeability of the nuclear membrane as determined with electrical methods. *Protoplasmatologia-Handbuch der Protoplasmaforschung.* 5(2):26–34.
35. Ito, S., and W. R. Loewenstein. 1965. Permeability of a nuclear membrane: changes during normal development and changes induced by growth hormone. *Science* (*Wash. DC*). 150:909–910.
36. Kanno, Y., R. F. Ashman, and W. R. Loewenstein. 1965. Nucleus and cell membrane conductance in marine oocytes. *Exp. Cell Res.* 39:184–189.
37. Loewenstein, W. R., Y. Kanno, and S. Ito. 1966. Permeability of the nuclear membrane. *Ann. NY. Acad. Sci. USA* 137:708–716.
38. Giulian, D., and E. G. Diacumakos. 1977. The electrophysiological mapping of compartments within a mammalian cell. *J. Cell. Biol.* 72:86–103.
39. Overbeek, J. Th. G. 1956. The Donnan equilibrium. *Prog. Biophys. Biophys. Chem.* 6:57–85.
40. Yoon, B. J., and A. M. Lenhoff. 1992. Computation of the electrostatic interaction energy between a protein and a charged surface. *J. Phys. Chem.* 96:3130–3134.

41. Burke, B. 1990. The nuclear envelope and nuclear transport. *Curr. Opin. Cell Biol.* 2:514–520.
42. Karin, M. 1991. Signal transduction and gene control. *Curr. Opin. Cell Biol.* 3:467–473.
43. Nigg, E. A., P. A. Baeuerle, and R. Lührmann. 1991. Nuclear import-export: in search of signals and mechanisms. *Cell.* 66:15–22.
44. Davis, L. I. 1992. Control of nucleocytoplasmic transport. *Curr. Opin. Cell. Biol.* 4:424–429.
45. Dingwall, C., and R. Laskey. 1992. The nuclear membrane. *Science (Wash. DC).* 258:942–947.
46. Bustamante, J. O., and D. Jachimowicz. 1988. Cryopreservation of human heart cells. *Cryobiology.* 25:394–408.
47. Bustamante, J. O., T. Watanabe, and T. F. McDonald. 1982. Non-specific proteases: a new approach to the isolation of adult cardiocytes. *Can. J. Physiol. Pharmacol.* 60:997–1002.
48. Bustamante, J. O., T. Watanabe, and T. F. McDonald. 1981. Single cells from adult mammalian heart isolation procedure and preliminary electrophysiological studies. *Can. J. Physiol. Pharmacol.* 59:907–910.
49. Bustamante, J. O. 1991. An inexpensive inverted microscope for patch-clamp and other electrophysiological studies at the cellular level. *Pflügers Arch.* 418:608–610.
50. Nam, S. C., and P. E. Hockberger. 1992. Divalent ions released from stainless steel hypodermic needles reduce neuronal calcium currents. *Pflügers Arch.* 420:106–108.
51. Bustamante, J. O. 1988. A system for the automated data-acquisition of fast transient signals in excitable membranes. *Int. J. Biomed. Comput.* 22:273–283.
52. Hamill, O. P., A. Marty, E. Neher, B. Sakmann, and F. J. Sigworth. 1981. Improved patch-clamp techniques for high-resolution current recording from cells and cell-free membrane patches. *Pflügers Arch.* 391:85–100.
53. Sakmann, B., and E. Neher. 1983. Single-Channel Recording. Plenum Press, New York. 503 pp.
54. Gerdes, A. M., M. C. Morales, V. Handa, J. A. Moore, and M. R. Alvarez. 1991. Nuclear size and DNA content in rat cardiac myocytes during growth, maturation and aging. *J. Mol. Cell. Cardiol.* 23:833–839.
55. Hille, B. 1992. Ionic Channels of Excitable Membranes. Sinauer Associates, Sunderland, MA. 607 pp.
56. Wonderlin, W. F., and R. J. French. 1991. Ion channels in transit: voltage-gated Na and K channels in axoplasmic organelles of the squid Loligo pealei. *Proc. Natl. Acad. Sci. USA.* 88:4391–4395.
57. Auerbach, A. 1991. Single channel dose-response studies in single cell-attached patches. *Biophys. J.* 60:660–670.
58. Hakes, D. J., and R. Berezney. 1991. Molecular cloning of matrin F/G: a DNA binding protein of the nuclear matrix that contains putative zinc finger motifs. *Proc. Natl. Acad. Sci. USA.* 88:6186–6190.
59. Wu, F. Y.-H. 1990. The intrinsic zinc ions of RNA polymerases and transcription factor. *In* Structure and Function of Nucleic Acids and Proteins. F. Y.-H. Wu and C.-W. Wu, editors. Raven Press, New York. 37–54.
60. Pavletich, N. P., and C. O. Pabo. 1991. Zinc finger-DNA recognition: crystal structure of a Zif268-DNA complex at 2.1. *Science (Wash. DC).* 252:809–817.
61. Boman, A. L., M. R. Delannoy, and K. L. Wilson. 1992. GTP hydrolysis is required for vesicle fusion during nuclear envelope assembly in vitro. *J. Cell Biol.* 116:281–294.
62. Adam, S. A., R. S. Marr, and L. Gerace. 1990. Nuclear protein import in permeabilized mammalian cells requires soluble cytoplasmic factors. *J. Cell Biol.* 111:807–816.
63. Newmeyer, D. D., and D. J. Forbes. 1990. An N-ethylmaleimide-sensitive cytosolic factor necessary for nuclear protein import: requirement in signal-mediated binding to the nuclear pore. *J. Cell Biol.* 110:547–557.
64. Spiegel, A. M. 1992. G proteins in cellular control. *Curr. Opin. Cell Biol.* 4:203–211.
65. Wong, I., and T. M. Lohman. 1992. Allosteric effects of nucleotide cofactors on *Escherichia coli* Rep helicase-DNA binding. *Science (Wash. DC).* 256:350–355.